

# Stiffness and compressive strength of a stabilized soil cured under stress

L. Pigeot, F. Dermenonville  
*Egis, Seyssin, France*

**N. Dufour**, H. Calissano, L. Batilliot  
*GeoCoD, Cerema, Aix-en-Provence, France*

A. Loukili  
*GeM, Ecole Centrale de Nantes, Nantes, France*

**ABSTRACT:** Linear transport infrastructure projects involve movements of large volumes of soil. In this context embankments built in stabilized soils can be higher than 10 meters. Actual's standards for laboratory testing don't take into consideration the depth, and therefore the pressure, at which stabilized soils are placed while they are curing. Therefore, the appropriate characterization of these soils requires the laboratory-made soil specimen to be subjected to curing stress. For this, a silty soil is stabilized with 1% lime and 5% cement and then compacted to produce soil specimens. They are then placed in standardized curing conditions (20°C and atmospheric pressure) or cured under stresses (20°C and 300 kPa) for 7, 28 or 90 days. Using P and S waves velocity measurement, the Young's and shear moduli of the specimens are calculated at each time and for each curing condition. Then these specimens are subjected to uniaxial compressive strength (UCS) tests, which is a major criterion in validating a stabilization choice for a soil. The waves velocity results show that the increase in moduli depends on the increase in curing time and curing pressure. These evolutions can be predicted accurately up to 90 days with the help of power laws based on measurements conducted after 7 days of curing. The study reveals that moduli are 20% higher when the specimens were under curing stress. In contrast the UCS values are not significantly influenced by the curing stress. This is partly explained by the deconfinement subjected to by the specimens before the tests. There is a linear relationship between the Young's and shear modulus obtained by the elastic waves propagation and the UCS value of each specimen. This relationship makes it possible to predict UCS of the specimens from non-destructive measurements which can be carried out throughout the curing.

**KEYWORDS:** stabilised soil, curing stress, elastic waves, uniaxial compressive strength

## 1 INTRODUCTION

The transport sector is a major contributor to carbon emissions. To address this, it is essential to promote a modal shift toward low-carbon alternatives such as rail and inland waterways. These infrastructures must be designed sustainably, meaning they should be dimensioned to anticipate future freight volumes and built with innovative, environmentally friendly materials. Developing such large-scale projects often involves constructing earthworks, which calls for a sustainable approach i.e. reusing excavated materials and minimizing the import of new resources. However, since local soils may have insufficient mechanical properties, chemical stabilization (using lime and eco-friendly hydraulic binders rich in slag or fly ash) and mechanical compaction techniques are commonly employed.

Technical guidelines (LCPC/SETRA, 2000) specify laboratory curing conditions for treated soils. Mechanical performance is typically assessed through uniaxial compressive strength (UCS) tests, as UCS tends to increase with curing time and treatment content. Combining lime with hydraulic binders is often chosen to achieve the required UCS levels. Additionally, the velocity of elastic P and S waves is widely used to monitor the evolution of soil stiffness during curing, providing complementary insights to UCS tests.

However, discrepancies have been observed between the properties measured on *in situ* core samples and those determined on reconstituted laboratory specimens (Clough et al., 1981). As early as the 1980s, studies on cemented sands revealed that laboratory tests often underestimated strength because they did not replicate the *in situ* confining pressures, especially at greater depths. To address this, protocols applying a "curing stress" i.e. a pressure matching the depth-related

confinement, were developed. It has since become common practice for deep soil mixing columns and cemented paste backfill (CBP) in mining, where curing pressures can reach several MPa (Cui & Fall, 2016; Shunman et al., 2021).

In contrast, the effect of curing stress on fine stabilized soils has been less explored. This study therefore proposes an experimental protocol that subjects laboratory specimens to a curing pressure of 300 kPa, simulating a depth of 15 meters, maintained for 7, 28, and 90 days in triaxial cells. The evolution of mechanical properties is tracked through UCS tests and measurements of elastic wave propagation, offering a practical and cost-effective way to assess the benefits of curing stress on stabilized soils.

## 2 EXPERIMENTAL PROGRAM

### 2.1 Materials

This study focuses on cemented soil specimens prepared from a mixture of soil, lime, and cement. The soil was excavated in northern France. A laser diffraction particle size analysis was performed on the fraction passing the 0.2 mm sieve, revealing that 80% of the particles were smaller than 0.08 mm, with a maximum grain size of 0.145 mm with a composition of approximately 81.4% silt, 11.0% clay, and 7.6% sand.

Additional characterization tests, including the blue methylene value (VBS = 2.2 g/100g) and Atterberg limits (LL = 28%, PL = 21%, PI = 7%), allowed the soil to be classified as ML (silt of low plasticity) under the Unified Soil Classification System (USCS, ASTM D2488, 2020).

The amounts of lime and hydraulic binder incorporated into the silt were 1% and 5% respectively, by dry weight of soil. This dosage was selected because it is commonly used in

geotechnical engineering and earthworks, making the study representative of most real-world projects. The lime consisted of approximately 90% quicklime (CaO), 7% portlandite (Ca(OH)<sub>2</sub>), 3% larnite, and traces of calcite (CaCO<sub>3</sub>), with a measured specific surface area of 6550 cm<sup>2</sup>/g. The hydraulic binder can be classified as a CEM III/A type cement (comprising 35% Portland cement clinker and 65% blast furnace slag).

## 2.2 Preparation of specimens for testing

To establish the target density and moisture content for specimen compaction, a Standard Proctor test was performed. This analysis determined the Optimum Moisture Content (OMC) and maximum dry density for the silt mixture stabilized with 1% lime and 5% cement. The maximum dry density was found to be 1.75 Mg/m<sup>3</sup>, corresponding to an OMC of 17.5%.

Specimens were statically compacted in a single layer (Serratrice, 2018) at  $w = \text{OMC} + 1\%$  until 96% of optimal density was reached (around 19.70 kN/m<sup>3</sup>). The result are specimens of 5 cm in diameter and 10 cm in height. The chosen compaction allows to obtain a good repeatability of the soil specimens. This allows to be able to compare them after their curing assuming that the differences observed are only the results of the times and curing conditions compared.

## 2.3 Curing and testing conditions

Table 1 summarizes the stabilized silty specimens along with their respective curing conditions and durations (7, 28, or 90 days). Some specimens were cured under standard conditions recommended by the guidelines: sealed in airtight packaging (plastic film and aluminum foil) and stored at a controlled temperature of 20°C under atmospheric pressure (LCPC/SETRA, 2000). These specimens are labeled N- (curing time) for “Normalized” conditions. Specimens designed to simulate treated soil placed at depth are labeled C- (curing time) for “Curing stress.” They were cured in a triaxial cell under an isotropic stress of 300 kPa at 20°C, with open drains, wet filter papers, and porous stones. After curing under confinement, the specimens were removed from the triaxial cells for weighing and length measurement.

Elastic wave propagation tests were then performed on each specimen before uniaxial compressive strength (UCS) tests, allowing these successive measurements since the wave tests are non-destructive. A minimum of three specimens was prepared for each curing duration and pressure to ensure repeatability and reliability of the test results. A total of 19 specimens were tested. The testing procedures are detailed in the following sections.

Table 1. Specimens curing and testing conditions.

Curing condition	Curing time (days)		
	7	28	90
Normalized cure	N-7	N-28	N-90
Curing stress	C-7	C-28	C-90

## 3 EXPERIMENTAL METHODS

### 3.1 P and S waves velocities measurement

The measurement of P- and S-wave ultrasonic velocities was performed. This experimental method involves transmitting an ultrasonic wave through a soil specimen and recording the time it takes to propagate. These non-destructive tests were carried out under unconfined conditions at atmospheric pressure. A Pundit-Lab ultrasonic analyzer by Proceq was used, equipped

with transducers for P- and S-waves. For P-wave measurements, a conductive gel was applied to opposite faces of the specimen to enhance contact between the soil and the piezoelectric sensors. These sensors convert an electrical pulse into a mechanical wave on the transmitting side and reconvert it into an electrical signal on the receiving side. The P- and S-waves were transmitted at frequencies of 54 kHz and 37 kHz, respectively, with pulse periods of 9.3 μs and 13.5 μs. These parameters were determined by the specifications of the testing equipment.

### 3.2 Uniaxial compressive strength tests

Uniaxial compressive strength (UCS) tests are used to assess the mechanical behavior of soil specimens under static loading up to failure. During testing, the specimen was positioned between a plexiglass base and cap, with wet filter papers to ensure uniform contact, and enclosed in a seamless neoprene membrane. It was then placed in a press equipped with a 25 kN load cell. The test was conducted by applying a load at a constant displacement rate of 0.004 mm/min. Loading began upon establishing contact with the specimen, corresponding to an initial force of approximately 0.005 kN.

## 4 RESULTS AND DISCUSSIONS

### 4.1 Young modulus and shear modulus prediction as function of time

As shown by Equation (1), the P- and S-wave velocity measurements ( $V_p$  and  $V_s$ ) were used to calculate the Young's shear moduli ( $E$  and  $G$ ) and the Poisson's ratio  $\nu$  of the tested specimens.

$$G = \rho V_s^2 \quad \text{and} \quad E = \rho V_s^2 \frac{3V_p^2 - 4V_s^2}{V_p^2 - V_s^2} \quad (1)$$

$$\nu = \frac{(V_p^2 - 2V_s^2)}{2(V_p^2 - V_s^2)} \quad (2)$$

Figures 1 and 2 illustrate how these moduli evolved over time. The increase was more pronounced between 7 and 28 days than between 28 and 90 days of curing. Specimens cured under confined conditions exhibited higher moduli than those cured under standard conditions. Specifically, the difference in Young's modulus between curing conditions was around 20% and remained roughly constant from 7 to 90 days. For the shear modulus, the difference was about 20% after 7 days, increasing to 25% between 28 and 90 days.

One objective of this study was to predict the behavior of stabilized silty soil when placed at depth in an embankment. Previous studies have modeled the evolution of soil properties shortly after binder addition (Toohey & Mooney, 2012). This approach, adapted for predicting the maximum value shear modulus of lime and cement stabilized silt (Pigeot et al., 2024), was used here to predict the evolution of Young's and shear moduli (Equation (3)).

$$E(t) = E_{t_1} \left( \frac{t}{t_1} \right)^\alpha \quad \text{or} \quad G(t) = G_{t_1} \left( \frac{t}{t_1} \right)^\alpha \quad (3)$$

In this model,  $E(t)$  and  $G(t)$  represent the moduli at time  $t$ ,  $E_{t_1}$  and  $G_{t_1}$  at a reference time  $t_1$ . The empirical  $\alpha$  parameter was determined specifically for this soil and this treatment based on experimental results. In this article,  $t_1$  is set at 7 days because this is the first curing time at which measurements were taken, but the proposed equation can be adapted to other curing times.

The prediction curves in Figures 1 and 2 show that this power law accurately described the evolution of G and E up to 90 days for both confined and standard curing. A single  $\alpha$  value of 0.31 (Table 2) was used for all curves. The excellent fit of this model is confirmed by  $R^2$  values close to 1.

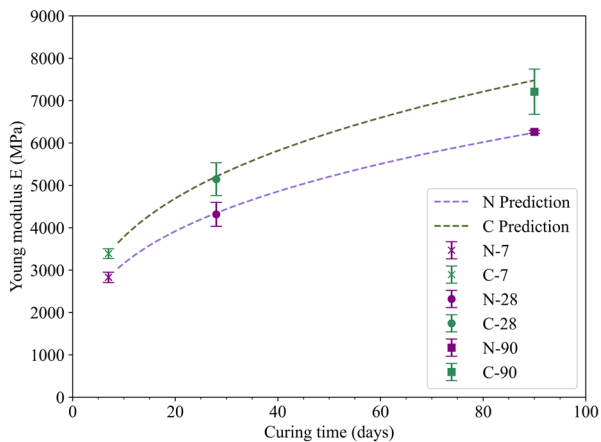


Figure 1. Evolution of Young modulus measured on normalized and curing stress specimens: comparison of experimental results and prediction.

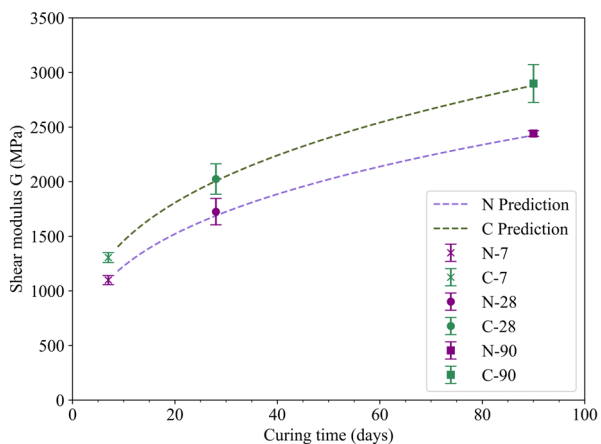


Figure 2. Evolution of shear modulus measured on normalized and curing stress specimens: comparison of experimental results and prediction.

Table 2. Evolution of the  $\alpha$  and  $R^2$  parameters between the experimental results and the predictions of the E and G moduli calculated from the elastic wave velocity measurements.

Curing condition	Shear Modulus		Young modulus	
	$\alpha$	$R^2$	$\alpha$	$R^2$
Normalized cure	0,31	0,99	0,31	0,99
Curing stress	0,31	0,99	0,31	0,96

Poisson's ratio, which reflects the compressibility of a material, can be calculated from the measured P wave and S wave velocities (Equation 2). As shown in Figure 3, Poisson's ratio exhibits a significant decrease between 7 and 28 days for both curing conditions. Beyond 28 days, the values tend to stabilize around 0.26. This stabilization of Poisson's ratio could be validated at a later stage with an experimental campaign involving longer curing times.

This trend indicates that the stabilized silt becomes progressively less compressible and stiffer with increasing curing time.

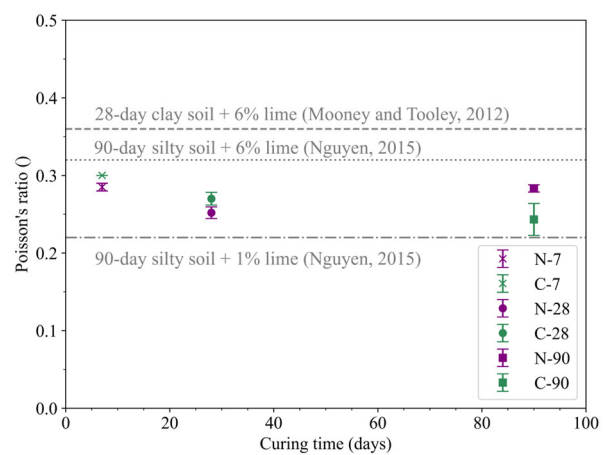


Figure 3. Poisson's ratio evolution as function of time.

#### 4.2 Uniaxial compression strength

To better illustrate the evolution of UCS, the measured values are plotted over time in Figure 4. This graph indicates that the average UCS values are comparable under both curing conditions. For specimens cured under standard conditions, the UCS values of the silt stabilized with lime and hydraulic binder align well with those reported in the literature for similar soils and treatments (Cabane, 2004). The absence of a significant difference due to curing stress suggests that the duration of confinement may not have been sufficient for the cementitious bonds between soil aggregates to develop enough strength to resist deconfinement. Testing at atmospheric pressure may cause slight deterioration and could reduce the measured UCS.

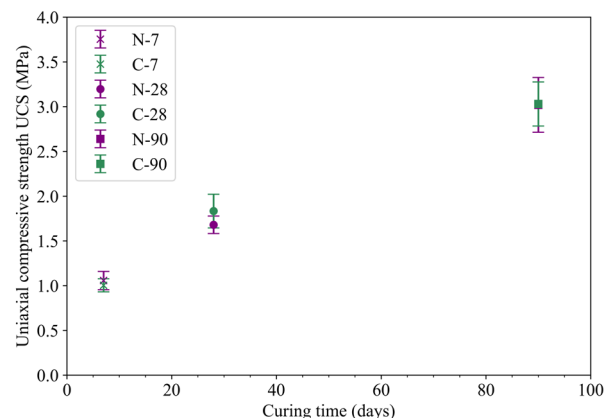


Figure 4. Effect of curing stress and time on uniaxial compressive strength (UCS) of stabilized soil specimens.

#### 4.3 Relation between modulus calculated from waves propagations and uniaxial compression strength (UCS)

Elastic wave propagation measurements and UCS tests were conducted sequentially on the same specimens from the experimental campaign. The results indicate linear relationships between UCS and both Young's and shear moduli, as illustrated in Figures 5 and 6.

These linear correlations, derived from graphical analyses, are summarized in Tables 3 and 4. The  $R^2$  values for specimens subjected to curing stress are close to 1, demonstrating an excellent fit to the experimental data.

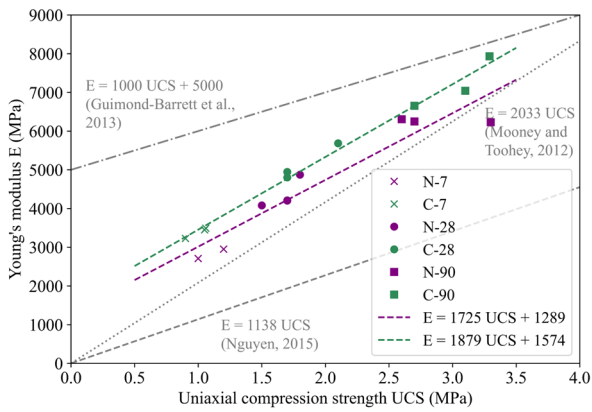


Figure 5. Young Modulus measured from waves velocities as function of unconfined compression strength UCS.

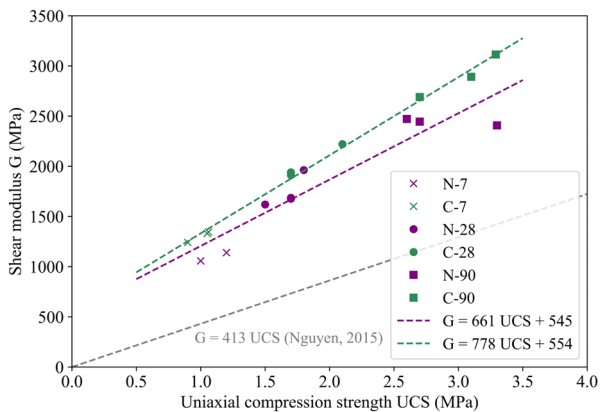


Figure 6. Shear modulus measured from waves velocities as function of UCS.

Tables 3 and 4 further shows that the  $R^2$  values are higher for specimens cured under confinement than for those cured under standard conditions. This suggests that achieving similar relationships between E, G, and UCS would require higher UCS values under confined curing. The regression lines obtained are valuable because they link destructive tests (UCS) with non-destructive wave velocity measurements, enabling the prediction of UCS over the curing period for specimens cured under standard conditions. However, for specimens cured under stress, UCS predictions may be underestimated due to microstructural alterations caused by unloading.

Table 3. Linear relation between Young's modulus calculated from the elastic wave velocity measurements and UCS.  $R^2$  parameters between the experimental results and the relations.

Curing condition	Linear relation	$R^2$
Normalized cure	$E = 1725 \text{ UCS} + 1289$	0,90
Curing stress	$E = 1879 \text{ UCS} + 1574$	0,99

Table 4. Linear relation between shear modulus calculated from the elastic wave velocity measurements and UCS.  $R^2$  parameters between the experimental results and the relations.

Curing condition	Linear relation	$R^2$
Normalized cure	$G = 661 \text{ UCS} + 545$	0,88
Curing stress	$G = 778 \text{ UCS} + 554$	0,99

## 5 CONCLUSIONS

This study highlights the interest of applying a confining pressure during the curing of treated soil specimens in the laboratory, particularly when these soils will be placed at depth, such as in high embankments for linear transport

infrastructures. To investigate this, two series of mechanical tests were performed on specimens cured for 7, 28, and 90 days: one under standard conditions (20°C, atmospheric pressure) and the other under a confining pressure of 300 kPa in a triaxial cell. Non-destructive P- and S-wave velocity measurements were followed by uniaxial compression tests on the same specimens. Results show that wave velocities and thus E and G moduli increase over time, following a power law, with values about 10–20% higher after curing under stress. Poisson's ratio decreases initially, stabilizing around 0.26. The largest mechanical gains occur within the first 7 days, consistent with hydration kinetics. While confined curing slightly improves UCS, testing at atmospheric pressure may induce minor specimen damage. Importantly, deconfinement does not appear to affect stiffness. A linear relationship was observed between moduli and UCS up to 90 days, enabling UCS prediction from non-destructive tests. Furthermore, it would be interesting to extend the experimental campaign to include different soils and treatments. It would also be possible to take measurements on test specimens cored from high stabilized embankments.

## 6 ACKNOWLEDGEMENTS

The research was supported by the Ecole Centrale de Nantes, Cerema institution and EGIS Géotechnique SE.

## 7 REFERENCES

- ASTM D2488 (2020). Practice for Classification of Soils for Engineering Purposes (Unified Soil Classification System). ASTM International. <https://doi.org/10.1520/D2487-17E01>
- Cabane, N. (2004). Sols traités à la chaux et aux liants hydrauliques : Contribution à l'identification et à l'analyse des éléments perturbateurs de la stabilisation [Thèse de doctorat]. Université Jean Monnet - Saint-Etienne.
- Clough, W., Sitar, N., & Bachus, R. (1981). Cemented Sands under Static Loading. *Journal of the Geotechnical Engineering Division*, 107, 799-817. <https://doi.org/10.1061/AJGEB6.0001152>
- Cui, L., & Fall, M. (2016). Mechanical and thermal properties of cemented tailings materials at early ages : Influence of initial temperature, curing stress and drainage conditions. *Construction and Building Materials*, 125, 553-563. <https://doi.org/10.1016/j.conbuildmat.2016.08.080>
- LCPC/SETRA. (2000). Traitement des sols à la chaux et/ou aux liants hydrauliques. Application à la réalisation des remblais et des couches de forme. Guide de Traitement des sols (GTS) (No. Réf. D9924; p. 79). LCPC.
- Pigeot, L., Dufour, N., Calissano, H., Dermenonville, F., & Soive, A. (2024). Influence of the curing stress effect on the stiffness degradation curve of a silt stabilized with lime and cement. *Engineering Geology*, 337, 107574. <https://doi.org/10.1016/j.enggeo.2024.107574>
- LCPC/SETRA. (2000). Traitement des sols à la chaux et/ou aux liants hydrauliques. Application à la réalisation des remblais et des couches de forme. Guide de Traitement des sols (GTS) (No. Réf. D9924; p. 79). LCPC.
- Serratrice, J.-F. (2018). Apport expérimental de la méthode de compactage statique des sols au laboratoire. *Revue Française de Géotechnique*, 156, 1. <https://doi.org/10.1051/geotech/2019001>
- Shunman, C., Wu, A., Yiming, W., & Wei, W. (2021). Coupled effects of curing stress and curing temperature on mechanical and physical properties of cemented paste backfill. *Construction and Building Materials*, 273, 121746. <https://doi.org/10.1016/j.conbuildmat.2020.121746>
- Toohy, N. M., & Mooney, M. A. (2012). Seismic modulus growth of lime-stabilised soil during curing. *Géotechnique*, 62(2), 161-170. <https://doi.org/10.1680/geot.9.P.122>